



Surface Modification of Activated Carbon Derived from Candlenut Shell (*Aleurites moluccana*) by HNO₃ and its Application as an Adsorbent of Methyl Orange Dyes



CrossMark

Safira Muliani, Muhammad Zakir*, St. Fauziah

Department of Chemistry, Faculty of Mathematics and Natural Sciences, University of Hasanuddin – Jl. Perintis Kemerdekaan, KM 10, Makassar, South of Sulawesi, 90245 Indonesia

Abstract

Surface modification of activated carbon from candlenut shell (*Aleurites moluccana*) was carried out with HNO₃ to adsorb methyl orange dye. The manufacture of activated carbon goes through four stages, namely carbonization at 700°C, activation with 10% H₃PO₄, modification with 4N HNO₃, and then pyrolysis at 300°C. Modified carbon was characterized by Fourier Transform Infrared (FTIR) and Scanning Electron Microscopy (SEM). Various contact times were used to study adsorption kinetics and various concentrations were used to study the adsorption isotherm pattern. The optimum time for adsorption of methyl orange dye was 40 minutes and the adsorption kinetic followed pseudo-second-order model. Adsorption isotherm of the activated carbon follows the Langmuir isothermal model with the adsorption capacity value of 17.668 mg.g⁻¹.

Keywords: activation, modification, adsorption, candlenut shell, methyl orange.

1. Introduction

Indonesia has an area that is used as an industrial area, tourism or for settlement. However, public awareness is still lacking to maintain the cleanliness of the surrounding environment, one of which is the aquatic environment. Pollution in the aquatic environment can be in the form of solid waste or liquid waste. The liquid waste comes from the textile, paper, paint and food industrial areas which use a lot of organic materials in their manufacture. It is generally believed that textile industries are one of such activities that utilize great number of water and thus yield a huge quantity of wastewater which mainly includes unconsumed chemicals and dyes [1].

One of the harmful substances commonly found in wastewater is synthetic dyes. Synthetic dyes are compounds formed from a combination of unsaturated organic substances with chromophores as color carriers and auxochromes as color binders with

fibers[2]. The synthetic dyes used are of various types such as acids, bases, azo, diazo, anthraquinone, and metal complex dyes [3]. One of the dyes found in industrial wastewater is methyl orange (MO). Methyl orange (MO) is an anionic dye that contains an azo group. This dye can cause hypertension and allergies [4].

The use of synthetic dyes in large doses often creates problems because of the concentrated color of the waste produced. Water bodies become unsightly, limited re-oxygenation capacity, and inhibition of sunlight will result in disruption of the photosynthesis process in aquatic ecosystems and the emergence of acute and chronic toxicity is a serious problem [5].

Various methods—such as filtration, flocculation, reverse osmosis and adsorption—have been attempted to handle liquid waste. Among them, adsorption is the best alternative to overcome dye pollution. Adsorption is a surface phenomenon where there is an interaction between two phases which causes the accumulation of particles on the surface of the

*Corresponding author e-mail: muh.zakir@science.unhas.ac.id (Muhammad Zakir)

Received date 08 July 2022; revised date 10 December 2022; accepted date 25 December 2022

DOI: [10.21608/EJCHEM.2022.149651.6476](https://doi.org/10.21608/EJCHEM.2022.149651.6476)

©2023 National Information and Documentation Center (NIDOC)

adsorbate [6]. The advantages of the adsorption method are that it has high efficiency to minimize unwanted compounds (toxic organic compounds), is easy to use, and can use various types of adsorbents [7].

Activated carbon is one type of adsorbent that can be applied to the adsorption method. The adsorbent in the form of activated carbon is used from agricultural waste which is composed of lignin, cellulose, and hemicellulose [8]. The production of activated carbon materials, especially from natural materials or biomass, attracts a lot of material research at this time. Activated carbon from biomass can also be applied as an electrochemical electrode for the valorisation of biomass waste [9]. Many activated carbons have been used as an adsorbent and was prepared from various wastes such as cocoa husk [10], plantain peel [11], bagasse [12], etc. Another waste that has the potential as an adsorbent is candlenut shell. According to Tambunan et al (2014), candlenut shell charcoal contains 76.315% bound carbon; 9.56% ash; 8.73% volatile compounds, and 5.35% water. Turmuzi et al (2004) reported that candlenut shells were high in lignocellulose content (49.22% holocellulose and 54.46% lignin) as a carbon source.

One of the efforts to maximize the function of activated carbon is not only from the surface area and pores but also on the carbon surface by modifying the surface [14]. In addition to the high surface area, the surface modification also influences the characteristics of carbon material. Modification of the activated carbon surface aims to create functional groups on the activated carbon surface [15].

Modification of the carbon surface by using an acid solution can generally be used to oxidize the carbon surface, improve the acid character, remove mineral elements and increase the hydrophilic properties of the activated carbon surface [16]. Research on modifying the surface of activated carbon has been carried out by Ramakrishnan et al (2009), where modifications were made with HNO_3 , H_2O_2 , and H_2SO_4 . The results showed that the modified activated carbon had an increase in the acid group and the most significant increase occurred in the activated carbon modified with HNO_3 . The modified activated carbon with HNO_3 showed an increase in the concentration of carboxyl groups, lactones (esters), and phenols (hydroxyl) which

increased its ability to interact with methyl orange. According to Gocke and Aktas (2014), the modified activated carbon with HNO_3 significantly increased the adsorbed dye because the carboxylate group produced could affect the adsorption of the dye.

Based on this description, this research was carried out to modify activated carbon from candlenut shells with HNO_3 as an adsorbent for Methyl Orange (MO) dye. Influential parameters such as contact time and concentration on the adsorption of dye by candlenut shell activated carbon will also be studied. The surface characterization using Scanning Electron Microscopy (SEM) to analyze the morphology of the carbon surface and Fourier Transform Infra Red (FT-IR) to analyze the functional groups on the surface.

2. Experimental

2.1 Material

Candlenut shell (taken from Leppanggeng Village, Lapriaja District, Bone Regency), distilled water, H_3PO_4 (Merck), HNO_3 (Merck), HCl (Merck), H_2SO_4 (Merck), Na_2CO_3 (Merck), NaHCO_3 (Merck), $\text{Na}_2\text{B}_4\text{O}_7 \cdot 10\text{H}_2\text{O}$ (Merck), NaOH (Merck), methyl orange (Merck), Phenolphthalein indicator (Merck), Red Methyl indicator (Merck), universal pH paper (E Merck), and Whatmann No.42 filter paper.

2.1 Tools

The tools that were used in this research are glassware commonly used in the laboratory such as petri dishes, 100 mesh size sieve, oven (SPNISOSFD type), thermometer, IKA Ceramag Midi stirrer hotplate, bar type (Fisher type 115), Oregon KJ-201BD orbital shaker, mortar, analytical balance (Shimadzu AW220), burette, plastic spray flask, UV-Vis Spectrophotometers (Shimadzu 20D+), Fourier Transform Infra Red (FT-IR) spectrophotometers (Shimadzu 820 IPC) and Scanning Electron Microscopy (SEM, JEOL JCM-7000).

2.3 General procedure

Preparation of Activated Carbon

The candlenut shell was washed with running water to remove the dirty particles attached to the candlenut shell surface and then dried in the sun and

then broken into small pieces. Then candlenut shell was carbonized in a furnace at a temperature of 700 °C for 1-2 hours without the flow of inert gas. This process will produce candlenut shell carbon. After carbonization, the carbon was cooled, pulverized, and then sieved with a size of 100 mesh. The preparation of activated carbon is carried out using chemical activators. Candlenut shell carbon is immersed in a 10% H_3PO_4 solution in a ratio of 5:1 (H_3PO_4 volume: carbon mass). The mixture was stirred and then allowed to stand for 24 hours at room temperature. After that, the mixture was filtered using a Buchner funnel with Whatman No. 42 filter paper, followed by washing with distilled water repeatedly until the pH was neutral which was measured using universal pH paper [19]. The carbon obtained is labeled KATK. Furthermore, the activated carbon of the

candlenut shell was dried in an oven at a temperature of 110 °C for 3 hours and then cooled in a desiccator.

Surface Modification

Surface modification of candlenut shell activated carbon mixed with an oxidizing solution of 4 N HNO_3 and KATK in a ratio of 5:1 (HNO_3 volume: KATK mass) was heated to boiling for 3.5 hours. After that, it was washed with distilled water repeatedly until the pH was neutral. Then dried in an oven for 24 hours at a temperature of 110 °C [16]. Furthermore, the modified candlenut shell activated carbon was pyrolyzed at a temperature of 300°C for 45 minutes and then cooled in a desiccator [20]. The modified carbon obtained is labeled KATM. The scheme of M of modified activated carbon as show at Figure 1.

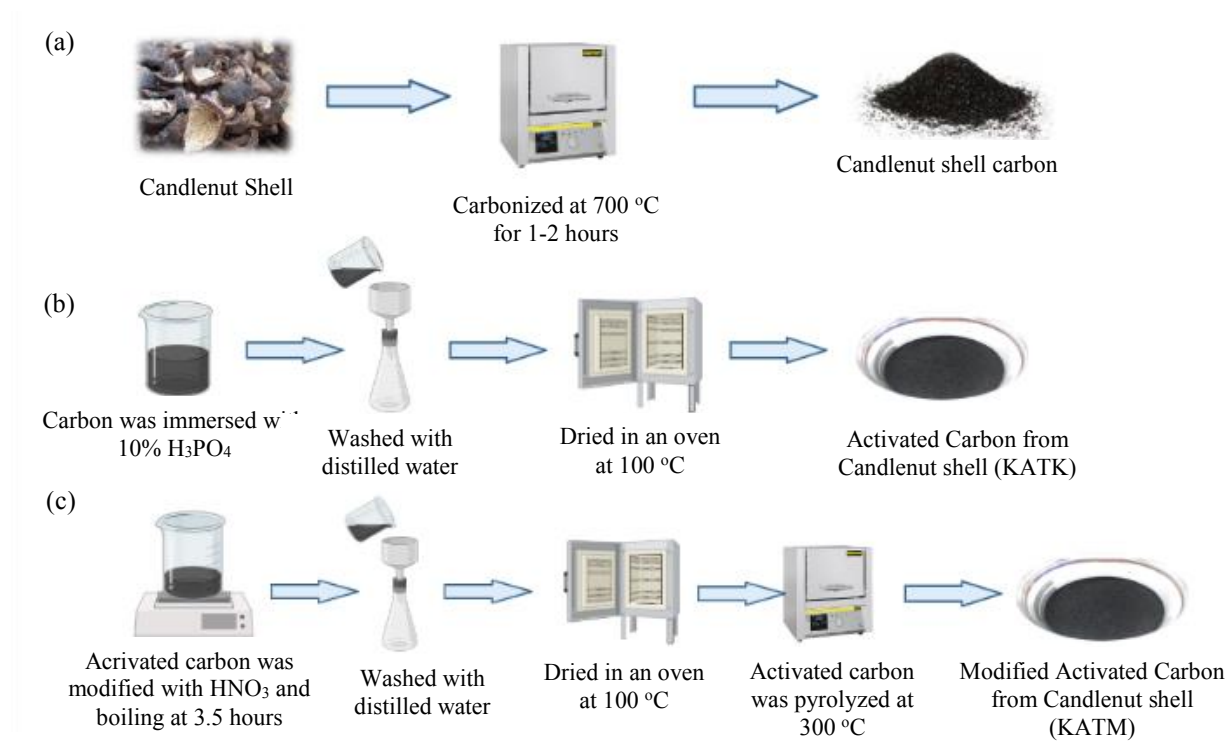


Figure 1. The scheme of making modified activated carbon with four stages (a) carbonization (b) activation with 10% H_3PO_4 (c) modification with HNO_3 and (d) pyrolysis at 300 °C

Adsorption

Methyl orange (Figure 2) dye adsorption process by modified carbon was studied using contact time and concentration conditions. Adsorption is studied based on contact time data and adsorption isotherms use concentration data.

MO stock solution was prepared at a concentration

of 1000 $mg.L^{-1}$ and diluted to give a suitable standard solution. Determination of contact time was performed with a concentration of MO 20 $mg.L^{-1}$, then 0.1 gram of KATM was put into 9 erlenmeyer and then contacted with 50 mL of methyl orange dye solution each. The mixture was stirred using an orbital shaker at a speed of 180 rpm with time

variations of 10, 15, 20, 25, 30, 35, 40, 45, and 50 minutes. Then the mixture was filtered and the filtrate obtained was measured for absorbance at the maximum wavelength with a UV-Vis spectrophotometer. Determination of adsorption capacity with 0.1 g KATM weighed and put into different erlenmeyer then mixed with various concentrations of 20, 25, 30, 40, 50, and 60 mg.L⁻¹ each was pipetted as much as 50 mL and then stirred with an orbital shaker at optimum contact time. Then filtered with whattman filter paper No. 42 and the obtained filtrate was measured using a UV-Vis spectrophotometer at a wavelength of 460 nm.

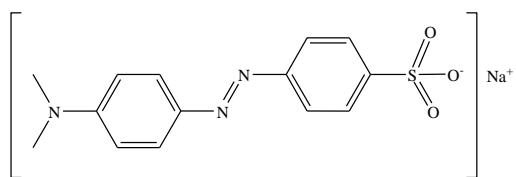


Figure 2. Structure of methyl orange (in the salt form)

MO adsorption (q) can be calculated from the concentration of methyl orange before and after being adsorbed with the formula:

$$q_t = \frac{C_o - C_e}{w} V \quad (1)$$

where q is the amount of methyl orange adsorbed (mg.g⁻¹), C_o is the initial concentration and C_e is the final concentration of methyl orange in solution (mg.L⁻¹), V is the volume of the solution (L), and W is the mass of the sorbent (g).

Study of Adsorption Kinetics and Isotherm Models

It is important to study the kinetics because both the adsorption rate (one of the efficiency criteria for bending adsorbents) and the adsorption mechanism can be deduced from kinetic studies [21]. The pseudo-first-order kinetic model proposed by Lagergren is based on the increase in the adsorbent adsorbed on the solid as a function of time, usually expressed by Equation 2:

$$\ln(q_e - q_t) = \ln q_e - k_1 t \quad (2)$$

Then a graph is made between $\ln(q_e - q_t)$ versus t , it can be calculated with the values of q_e and k_1 , where q_e is the amount of adsorbent adsorbed at equilibrium (mg.g⁻¹), q_t is the amount of adsorbent adsorbed at

time t , and k_1 is the rate constant first-order adsorption (min⁻¹). Meanwhile, the pseudo-second-order kinetics model is based on the adsorption rate in the solid phase, which is expressed by Equation 3:

$$\frac{t}{q_t} = \frac{1}{q_e^2 k_2} + \frac{t}{q_e} \quad (3)$$

Then a graph is made between (t/q_t) versus t , so that the values of q_e and k_2 can be calculated, where q_e is the amount of adsorbent adsorbed at equilibrium (mg.g⁻¹), q_t is the amount of adsorbent adsorbed at the time t (mg.g⁻¹) and k_2 is the second-order adsorption rate constant (g.mg⁻¹.min⁻¹).

The relationship between the concentration of the solute adsorbed on the solid and the concentration of the solution, at a constant temperature, is called isothermal adsorption. The adsorption isothermal equation commonly used is the one studied and developed by Freundlich and Langmuir [22]. The Freundlich isothermal is based on the assumption that adsorbents with heterogeneous surfaces are capable of adsorption. In the adsorption process, a Freundlich isothermal is used which is derived empirically with the form [23]:

$$\log q_e = \log K_f + \frac{1}{n} \log C_e \quad (4)$$

where q_e is the amount of adsorbed MO dye per gram of adsorbent (mg.g⁻¹), C_e is the concentration of the adsorbate at equilibrium (mg.L⁻¹), and K is the adsorption capacity (mg.g⁻¹), and n is the adsorption intensity.

Langmuir isothermal is based on the assumption that the maximum adsorption corresponds to a single layer of adsorbate molecules being adsorbed on the surface of the adsorbent, where the adsorption energy is constant and there is no movement of the adsorbate on the surface plane. The linear form of the Langmuir isothermal equation is shown in Equation 3 [27]:

$$\frac{C_e}{q_e} = \frac{1}{Q_o b} + \frac{C_e}{Q_o}$$

(5)

where C_e is the concentration of the adsorbate at equilibrium (mg.L⁻¹). q_e is the amount of adsorbed MO dye per gram of adsorbent (mg/g). Q_o is adsorption capacity (mg.g⁻¹) and b is adsorption intensity (L.mg⁻¹).

3. Result and Discussion

3.1 Characterization of KATM

KATM characterization was carried out to know the characteristics of KATM. The characterization was carried out by using several instruments such as FTIR and SEM. The carbon yield obtained in this study is 22,61-39,88%.

Fourier Transform Infra-Red (FTIR)

Characterization using FTIR to identify functional groups of modified candlenut shell activated carbon (KATM). The results of the IR absorption spectrum analysis can be seen in Figure 2.

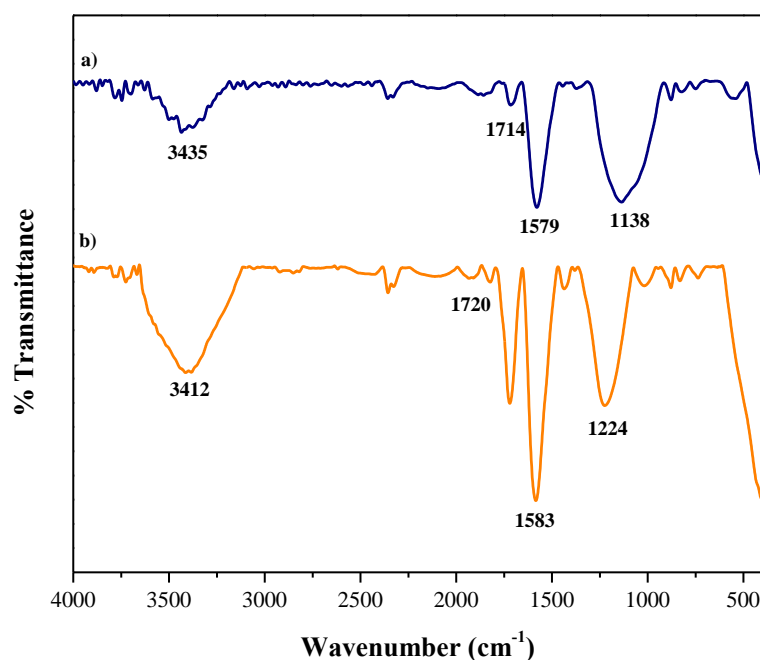


Figure3. Fourier Transform Infra Red (FT-IR) spectra of (a) KATK as activated carbon (b) KATM as modified activated carbon with HNO_3

Figure 3 shows the difference in transmittance from KATK and KATM. There is wave number in the area of 3435 cm^{-1} and 1138 cm^{-1} , namely in phenol. This is because the activation process using H_3PO_4 which can substitute the $-\text{OH}$ group to carbon (Figure 3(a)). In Figure 3(b) spectrum, there is a strong transmittance band in the 3412 cm^{-1} area which is widened indicating the presence of an $-\text{OH}$ group. Then it was strengthened by the strong transmittance in the 1224 cm^{-1} area, indicating the $-\text{OH}$ group derived from carboxylic acids. The transmittance band in the 1720 cm^{-1} region indicates the transmittance of the $\text{C}=\text{O}$ group from the carboxylic acid. The strong transmittance band in the 1583 cm^{-1} area indicates the presence of a $\text{C}=\text{C}$ group of aromatics. These results confirm that the KATM surface does possess oxygen-based functional groups which can be formed by acid treatment in which the amount of oxygen obtained depends on the method and the precursor used.

Scanning Electron Microscopy (SEM)

The results of SEM analysis show the characteristics based on the morphology of the modified candlenut shell activated carbon sample (KATM). Surface morphology of modified candlenut shell activated carbon (KATM) with HNO_3 and heating at a temperature of $300\text{ }^\circ\text{C}$ showed that the large pores formed were more visible and the pore sizes were uniform. This modification by using HNO_3 causes the diameter and total pore volume of the candlenut shell carbon to increase through the reaction of breaking the carbon chain on the KATM surface so that more pores are formed, as shown in Figure 4. Morphology of the modified candlenut shell activated carbon with HNO_3 and heating at a temperature of $300\text{ }^\circ\text{C}$ showed the best pore results compared to KATK. It can be seen that many pores formed are more visible and the pore size is uniform.

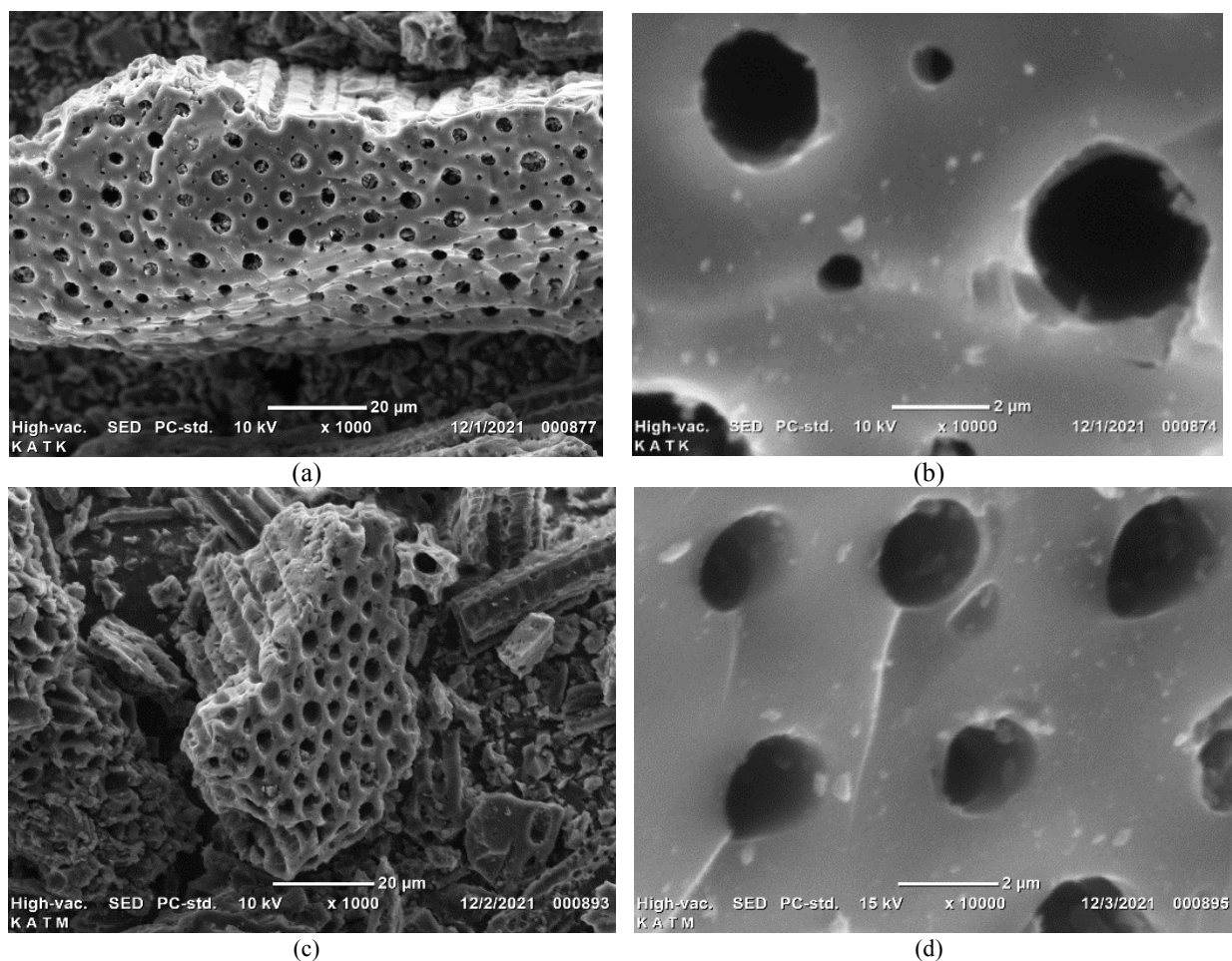


Figure 4. Surface morphology of (a) KATK 1000x (b) KATK 10000x (c) KATM 1000x (d) KATM 10000x using Scanning Electron Microscopy (SEM)

3.2 Adsorption

Effect of Contact Times and Adsorption Kinetics Models

Figure 5 shows an increase in the amount of methyl orange dye adsorbed between 10 minutes to 40 minutes. At a contact time of 10 minutes, the amount of dye adsorbed was 5.9886 mg.g^{-1} and then increased to a maximum contact time of 40 minutes with the adsorption of the dyestuff being 6.9201 mg.g^{-1} . From 40 minutes to 50 minutes there was a decrease in the amount of methyl orange adsorbed from the adsorption of 6.9201 mg.g^{-1} to 6.2206 mg.g^{-1}

¹. Thus, the optimum contact time of modified candlenut shell activated carbon (KATM) is 40 minutes with an adsorption of 6.9201 mg.g^{-1} . The decrease in dyes in determining the optimum contact time of KATM because the carbon has been saturated by the adsorbed molecule. This is because the surface of the adsorbent that has been filled with the adsorbate has been completely closed so that when the contact time is extended, there is no surface of the adsorbent that can absorb the adsorbate and can be released again [24].

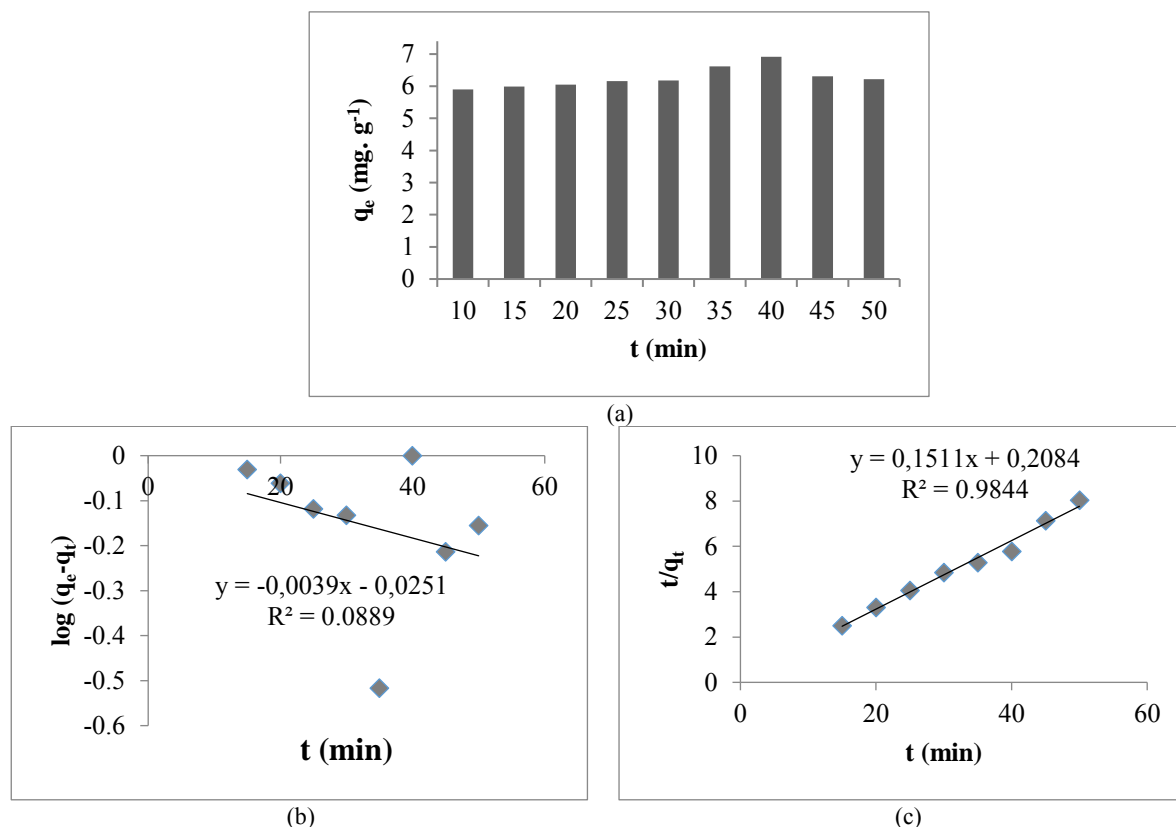


Figure 5. (a) Effect contact time on adsorption capacity (q_e) and adsorption kinetics of methyl orange: (b) pseudo-first-order (c) pseudo-second-order

Table 1

Summary of adsorption kinetic models obtained from Eq. (2) and Eq. (3) to $\log(q_e - q_t)$ vs t and t/q_t vs t plots for pseudo-first order and pseudo-second-order

Kinetic Models	Parameters	Values
Pseudo-first-order	k_1 (min^{-1})	0.0089
	R^2	0.0889
	q_e ($\text{mg}\cdot\text{g}^{-1}$)	0.94
Pseudo-second-order	k_2 ($\text{g}\cdot\text{mg}^{-1}\cdot\text{min}^{-1}$)	0.2084
	R^2	0.9844
	q_e ($\text{mg}\cdot\text{g}^{-1}$)	4.80

The amount of MO dye adsorbed on KATM in equilibrium can be calculated based on the linear equations of the pseudo-first-order and pseudo-second-order equations. Table 1 shows the comparison of pseudo-first-order reaction rates and pseudo-secondary reaction rates for the adsorption of MO dyes adsorbed on KATM. The correlation coefficient (R^2) can be calculated from the two equations. This is shown in Figure 5. The pseudo-first-order equation is $0.94 \text{ mg}\cdot\text{g}^{-1}$ ($R = 0.0889$) and the pseudo-second-order equation is $4.80 \text{ mg}\cdot\text{g}^{-1}$ ($R = 0.9844$). The pseudo-second-order correlation coefficient is close to 1 and the calculated q_e value is close to the experimental q_e value. This proves that

the adsorption of MO by KATM follows a pseudo-second-order reaction rate model. Table 1 above shows the comparison of pseudo-first-order and pseudo-second-order response constants for MO dye adsorption by KATM.

Effect of Concentration and Isotherm Adsorption Models

Figure 6 shows that the amount of methyl orange adsorbed by KATM increases with the increasing concentration of adsorbate. This is by Langmuir's theory which states that on the surface of the adsorbent, there are active groups that are proportional to the surface area of the adsorbent. The

amount of methyl orange absorbed will increase with the increase in the concentration of the dye as long as the active group of the adsorbent is not saturated [25]. The correlation coefficient of methyl orange dye adsorption by KATM tends to follow Langmuir isothermal as evidenced by the results of a linearity graph plot that is closer to 1, namely 0.9936 for KATM, this indicates that the adsorbent surface is

homogeneous where adsorption only occurs in a single layer (monolayer) [7]. Langmuir isothermal also shows that adsorption occurs chemically due to the formation of hydrogen bonds between the active groups on the surface of the adsorbent and the active groups on the adsorbate. The ratio of the value of the two isothermal models can be seen in Table 2.

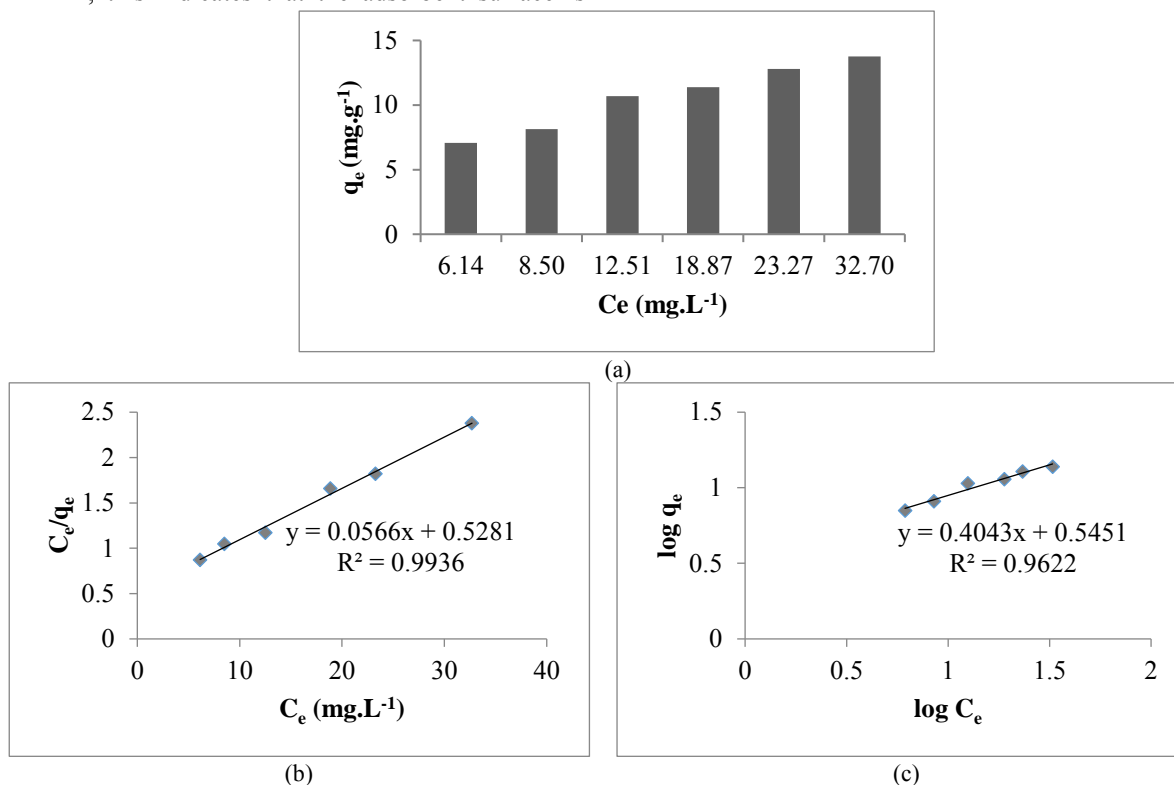


Figure6. (a) Effect of concentration on adsorption capacity (q_e) and adsorption isotherm model: (b) Langmuir Isotherm, and (c) Freundlich isotherm

Table 2

Summary of isotherm adsorption obtained from Eq. (4) and Eq. (5) to $\log (q_e - qt)$ vs t and t/qt vs t plots for pseudo-first order and pseudo-second-order

Isotherm Models	Parameters	Values
Langmuir	R^2	0.9936
	Q_0 (mg.g ⁻¹)	17.668
	b (L.mg ⁻¹)	0.1072
Freundlich	R^2	0.9622
	k (mg.g ⁻¹)	3.5083
	q_e (mg.g ⁻¹)	4.80

Table 3 shows the comparison of adsorption of methyl orange dye using various adsorbents. Annadurai (2002) reported that the carbon sourced from orange peel and banana peel yielded adsorption capacities of 15.8 mg.g⁻¹ and 17.2 mg.g⁻¹, respectively. This is different from the results of this

study which used candlenut shells as the carbon source, because candlenut shell has higher lignocellulose (49.22% holocellulose and 54.46% lignin) than orange peel and banana peel. In addition, a study conducted by Alqaragully (2014) using date of palm seeds as a carbon source to absorb methyl

orange dye of 3.07 mg.g⁻¹. This is different from the results of this study because the carbon used was modified with

HNO₃ so that the surface change of the activated carbon is effective for adsorption of methyl orange dye (Table 3).

Table 3

Summary of adsorption isotherm models obtained from Eq. (4) and Eq. (5) to $\log(qe-qt)$ vs t and t/qt vs t plots for pseudo-first order and pseudo-second-order

Carbon Source	Adsorption Isotherm	Adsorption Capacity (mg.g ⁻¹)	Reference
Orange peel	Langmuir	15,8	[7]
Banana peel	Freundlich	17,2	[7]
Dates Seeds	Langmuir	3,07	[26]
Candlenut shell	Langmuir	17,66	This study

4. Conclusions

The optimum condition of contact time adsorption of the methyl orange dyes by the KATM is obtained at 40 minutes with an adsorption value of 4.80 mg.g⁻¹ and follows the pseudo-second-order adsorption kinetics model, whereas the adsorption capacity for the KATM to the methyl orange dyes is 17.668 mg.g⁻¹ with the Langmuir isotherm model.

5. Conflicts of interest

We as authors declare that there is no conflict of interest in the publication of the article.

6. References

- [1] Failisnur, S. (2017). Reuse of liquid waste from textile dyeing with natural dyes gambier (*Uncaria gambir* Roxb.) for cotton yarn dyeing. *ARPN Journal of Engineering and Applied Sciences*, 12, 5313-5318.
- [2] Khan, R., Bhawana, P., & Fulekar, M. H. (2013). Microbial decolorization and degradation of synthetic dyes: a review. *Reviews in Environmental Science and Bio/Technology*, 12(1), 75-97.
- [3] Hajati, S., Ghaedi, M., Karimi, F., Barazesh, B., Sahraei, R., & Daneshfar, A. (2014). Competitive adsorption of Direct Yellow 12 and Reactive Orange 12 on ZnS: Mn nanoparticles loaded on activated carbon as novel adsorbent. *Journal of Industrial and Engineering Chemistry*, 20(2), 564-571.
- [4] Obeid, L., Bée, A., Talbot, D., Jaafar, S. B., Dupuis, V., Abramson, S., ... & Welschbillig, M. (2013). Chitosan/maghemite composite: A magsoorbent for the adsorption of methyl orange. *Journal of colloid and interface science*, 410, 52-58.
- [5] Ali, H. (2010). Biodegradation of synthetic dyes—a review. *Water, Air, & Soil Pollution*, 213(1), 251-273.

- [6] Dąbrowski, A. (2001). Adsorption—from theory to practice. *Advances in colloid and interface science*, 93(1-3), 135-224.
- [7] Annadurai, G., Juang, R. S., & Lee, D. J. (2002). Use of cellulose-based wastes for adsorption of dyes from aqueous solutions. *Journal of hazardous materials*, 92(3), 263-274.
- [8] Adegoke, K. A., & Bello, O. S. (2015). Dye sequestration using agricultural wastes as adsorbents. *Water Resources and Industry*, 12, 8-24.
- [9] Dubey, P., Shrivastav, V., Maheshwari, P. H., & Sundriyal, S. (2020). Recent advances in biomass derived activated carbon electrodes for hybrid electrochemical capacitor applications: Challenges and opportunities. *Carbon*, 170, 1-29.
- [10] Odubiyi, O. A., Awoyale, A. A., & Eloka-Eboka, A. C. (2012). Wastewater treatment with activated charcoal produced from cocoa pod husk. *Int. J. Environ. Bioener*, 4(3), 162-175.
- [11] Gupta, H., & Gupta, B. (2016). Adsorption of polycyclic aromatic hydrocarbons on banana peel activated carbon. *Desalination and Water Treatment*, 57(20), 9498-9509.
- [12] Mohan, D., & Singh, K. P. (2002). Single-and multi-component adsorption of cadmium and zinc using activated carbon derived from bagasse—an agricultural waste. *Water research*, 36(9), 2304-2318.
- [13] Turmuzi, M., Daud, W. R. W., Tasirin, S. M., Takriff, M. S., & Iyuke, S. E. (2004). Production of activated carbon from candlenut shell by CO₂ activation. *Carbon*, 42(2), 453-455.
- [14] Mangun, C. L., Benak, K. R., Economy, J., & Foster, K. L. (2001). Surface chemistry, pore sizes and adsorption properties of activated carbon fibers and precursors treated with ammonia. *Carbon*, 39(12), 1809-1820.
- [15] Bhatnagar, A., Hogland, W., Marques, M., & Sillanpää, M. (2013). An overview of the modification methods of activated carbon for its water treatment applications. *Chemical Engineering Journal*, 219, 499-511.
- [16] Shim, J. W., Park, S. J., & Ryu, S. K. (2001). Effect of modification with HNO₃ and NaOH on metal adsorption by pitch-based activated carbon fibers. *Carbon*, 39(11), 1635-1642.
- [17] Ramakrishnan, K., & Namasivayam, C. (2009). Development and characteristics of activated carbons from *Jatropha* husk, an agro industrial

- solid waste, by chemical activation methods. *J. Environ. Eng. Manage*, 19(3), 173-178.
- [18] Gokce, Y., & Aktas, Z. (2014). Nitric acid modification of activated carbon produced from waste tea and adsorption of methylene blue and phenol. *Applied Surface Science*, 313, 352-359.
- [19] Prahas, D., Kartika, Y., Indraswati, N., & Ismadji, S. J. C. E. J. (2008). Activated carbon from jackfruit peel waste by H₃PO₄ chemical activation: Pore structure and surface chemistry characterization. *Chemical Engineering Journal*, 140(1-3), 32-42.
- [20] Chen, D., Chen, X., Sun, J., Zheng, Z., & Fu, K. (2016). Pyrolysis polygeneration of pine nut shell: quality of pyrolysis products and study on the preparation of activated carbon from biochar. *Bioresource technology*, 216, 629-636.
- [21] Aljeboree, A. M., Alshirifi, A. N., & Alkaim, A. F. (2017). Kinetics and equilibrium study for the adsorption of textile dyes on coconut shell activated carbon. *Arabian journal of chemistry*, 10, S3381-S3393.
- [22] Jeppu, G. P., & Clement, T. P. (2012). A modified Langmuir-Freundlich isotherm model for simulating pH-dependent adsorption effects. *Journal of contaminant hydrology*, 129, 46-53.
- [23] Atkins, P.W. (1994) *Physical Chemistry Fifth Edition*, Oxford: Oxford University Press.
- [24] Lithoxoos, G. P., Labropoulos, A., Peristeras, L. D., Kanellopoulos, N., Samios, J., & Economou, I. G. (2010). Adsorption of N₂, CH₄, CO and CO₂ gases in single walled carbon nanotubes: A combined experimental and Monte Carlo molecular simulation study. *The Journal of Supercritical Fluids*, 55(2), 510-523.
- [25] Subbaiah, M. V., & Kim, D. S. (2016). Adsorption of methyl orange from aqueous solution by aminated pumpkin seed powder: Kinetics, isotherms, and thermodynamic studies. *Ecotoxicology and environmental safety*, 128, 109-117.
- [26] Alqaragully, M. B. (2014). Removal of textile dyes (maxilon blue, and methyl orange) by date stones activated carbon. *Int J Adv Res Chem Sci*, 1(1), 48-59.
- [27] Periasamy, K., & Namasivayam, C. (1995). Removal of nickel (II) from aqueous solution and nickel plating industry wastewater using an agricultural waste: peanut hulls. *Waste management*, 15(1), 63-68.